International Journal of Nanomedicine

Dovepress
open access to scientific and medical research

Open Access Full Text Article

ORIGINAL RESEARCH

$\alpha_v\beta_3$ integrin-targeted micellar mertansine prodrug effectively inhibits triple-negative breast cancer in vivo

This article was published in the following Dove Press journal:
International Journal of Nanomedicine
27 October 2017
Number of times this article has been viewed

Ping Zhong[1,2]
Xiaolei Gu[1,2]
Ru Cheng[1,2]
Chao Deng[1,2]
Fenghua Meng[1,2]
Zhiyuan Zhong[1,2]

[1]Biomedical Polymers Laboratory, [2]Jiangsu Key Laboratory of Advanced Functional Polymer Design and Application, College of Chemistry, Chemical Engineering and Materials Science, Soochow University, Suzhou, China

Abstract: Antibody-mertansine (DM1) conjugates (AMCs) are among the very few active targeting therapeutics that are approved or clinically investigated for treating various cancers including metastatic breast cancer. However, none of the AMCs are effective for the treatment of triple-negative breast cancers (TNBCs). Here, we show that cRGD-decorated, redox-activatable micellar mertansine prodrug (cRGD-MMP) can effectively target and deliver DM1 to $\alpha_v\beta_3$ integrin overexpressing MDA-MB-231 TNBC xenografts in nude mice, resulting in potent tumor growth inhibition. 3-(4,5-Dimethylthiazol-2-yl)-2,5-diphenyltetrazolium bromide (MTT) assays showed that cRGD-MMP had obvious targetability to MDA-MB-231 cells with a low half-maximal inhibitory concentration (IC_{50}) of 0.18 μM, which was close to that of free DM1 and 2.2-fold lower than that of micellar mertansine prodrug (MMP; nontargeting control). The confocal microscopy studies demonstrated that cRGD-MMP mediated a clearly more efficient cellular uptake and intracellular release of doxorubicin (used as a fluorescent anticancer drug model) in MDA-MB-231 cells. Notably, cRGD-MMP loaded with 1,1′-dioctadecyltetramethyl indotricarbocyanine iodide (DiR; a hydrophobic near-infrared dye) was shown to quickly accumulate in the MDA-MB-231 tumor with strong DiR fluorescence from 2 to 24 h post injection. MMP loaded with DiR could also accumulate in the tumor, although significantly less than cRGD-MMP. The biodistribution studies revealed a high DM1 accumulation of 8.1%ID/g in the tumor for cRGD-MMP at 12 h post injection. The therapeutic results demonstrated that cRGD-MMP effectively suppressed MDA-MB-231 tumor growth at 1.6 mg DM1 equiv./kg without causing noticeable side effects, as shown by little body weight loss and histological analysis. This MMP has appeared as a promising platform for potent treatment of TNBCs.

Keywords: breast cancer, reduction-sensitive, drug conjugates, micelles, cRGD

Introduction

Mertansine (DM1) is a powerful tubulin polymerization inhibitor that can effectively treat various malignancies, including breast cancer, melanoma, multiple myeloma and lung cancer.[1–3] The extremely high potency of DM1 renders it an ideal warhead in the development of antibody–drug conjugates (ADCs) for targeted tumor therapy.[4–6] In 2013, Kadcyla (ado-trastuzumab emtansine) that targets DM1 to HER2 was approved by the US Food and Drug Administration (FDA) for the treatment of patients with HER2-positive metastatic breast cancer.[7,8] The success of ado-trastuzumab emtansine has spurred intensive clinical development of novel ADCs based on DM1 but different antibodies for targeting to various tumors.[4,5,9] Undoubtedly, ADCs with DM1 warhead are among the most advanced active targeting cancer nanomedicines that

Correspondence: Ru Cheng; Zhiyuan Zhong
Jiangsu Key Laboratory of Advanced Functional Polymer Design and Application, College of Chemistry, Chemical Engineering and Materials Science, Soochow University, No 199 Ren'ai Road, Suzhou 215123, China
Tel/fax +86 512 6588 0098
Email rcheng@suda.edu.cn; zyzhong@suda.edu.cn

submit your manuscript | www.dovepress.com
Dovepress
http://dx.doi.org/10.2147/IJN.S146505

are expected to greatly improve the therapeutic outcomes of many refractory cancers.

None of the ADCs including ado-trastuzumab emtansine, however, can be used to treat triple-negative breast cancer (TNBC) that accounts for 12%–17% of globally diagnosed breast cancer. TNBC is a highly heterogeneous subtype of breast cancer that does not express, or expresses, low levels of estrogen receptor (ER), progesterone receptor (PR) and human epidermal growth factor receptor.[10–12] The lack of the above therapeutic receptors makes TNBC insensitive to hormone therapy such as Nolvadex® (tamoxifen) used in ER-positive cancer treatment and to trastuzumab (Herceptin®) commonly used for HER2-positive tumors.[13–15] TNBC remains a formidable challenge for current clinical practices.[16–18]

In contrast to ADCs, polymeric micellar nanomedicines that can be decorated with different targeting ligands are a more versatile treatment modality for cancer chemotherapy.[19–21] In the past few years, various micellar nanomedicines have been designed for targeted treatment of TNBC.[22–27] For instance, cetuximab-conjugated vitamin E d-α-tocopheryl polyethylene glycol succinate micelles were shown to increase efficacy of docetaxel (DTX) against TNBC.[22,23] Folate-targeted micelles loaded with orlistat exhibited better treatment of TNBC than free orlistat.[24] Aminoflavone-loaded EGFR-targeted unimolecular micelles based on poly(amidoamine)-polylactide-poly(ethylene glycol) were reported to significantly enhance treatment of orthotropic TNBC tumor as compared to the nontargeted counterpart and free aminoflavone.[25] The micellar nanoformulation of lipophilized bortezomib (BTZ) induced significantly better TNBC tumor accumulation and inhibition while lower adverse effects than free BTZ, leading to greatly improved mice survival rate.[28] It is interesting to note that in spite of clinical use of DM1 in the treatment of HER2-positive metastatic breast cancers, no systems based on DM1 have been developed for targeted treatment of TNBC.

We recently reported that cRGD-functionalized micellar mertansine prodrug based on poly(ethylene glycol)-*b*-(poly(trimethylene carbonate)-*graft*-SSDM1) (PEG-P(TMC-*g*-SSDM1)) mediated targeted treatment of $\alpha_v\beta_3$ integrin-overexpressed B16F10 melanoma.[29] Notably, cRGD-MMP has a significantly higher DM1 conjugation, better stability and improved tolerability as compared to ado-trastuzumab emtansine. The aim of the present work was to investigate therapeutic efficacy of cRGD-MMP toward MDA-MB-231 triple-negative breast tumor-bearing nude mice. cRGD peptide has shown a strong binding toward $\alpha_v\beta_3$ integrin-overexpressed MDA-MB-231 TNBC cells.[30–32] Interestingly, our results showed that cRGD-MMP can effectively target to and treat MDA-MB-231 cells in vivo. This micellar mertansine prodrug (MMP) has appeared as a promising platform for potent treatment of TNBC.

Materials and methods

Materials and characterizations

3-(4,5-Dimethylthiazol-2-yl)-2,5-diphenyltetrazolium bromide (MTT; Sigma-Aldrich Co., St Louis, MO, USA), 4′6-diamidino-2-phenylindole dihydrochloride (DAPI; Sigma-Aldrich Co.), 1,1′-dioctadecyltetramethyl indotricarbocyanine iodide (DiR; AAT Bioquest Inc., Sunnyvale, CA, USA) and doxorubicin (DOX) hydrochloride (Beijing ZhongShuo Pharmaceutical Technology Development Co., Ltd., Beijing, China) were used as received. PEG-P(TMC-*g*-SSDM1) and cRGD-PEG-P(TMC-*g*-SSDM1) were prepared by thiol–disulfide exchange reaction between DM1 with PEG-P(TMC-*co*-poly(pyridyldisulfide cyclic carbonate) [PDSC]) and Mal-PEG-P(TMC-*co*-PDSC) copolymers (Table 1), respectively, as in our previous report.[29] The characteristics of MMP and cRGD-MMP are summarized in Table 2. The amount of DM1 was determined by high-performance liquid chromatography (HPLC; Agilent 1260; Agilent Technologies, Santa Clara, CA, USA) using a mixture of acetonitrile and water (v/v =6/4) as a mobile phase with ultraviolet (UV) detection at 245 nm.

Cell culture and animals

MDA-MB-231 TNBCs that express a high level of $\alpha_v\beta_3$ integrins were obtained from the Type Culture Collection of the Chinese Academy of Sciences, Shanghai, China. MDA-MB-231 cancer cells were cultured in the Dulbecco's Modified Eagle's Medium (DMEM; Hyclone, Logan, Utah, USA) supplemented with 10% fetal bovine serum (FBS; Thermo Fisher Scientific, Waltham, MA, USA), 1% L-glutamine, antibiotics penicillin (100 IU/mL) and streptomycin (100 μg/mL; Jinuo Biomedical Technology, Hangzhou, Zhejiang, China) under 5% CO_2 at 37°C.

Table 1 Characterization of PEG-P(TMC-*co*-PDSC) and Mal-PEG-P(TMC-*co*-PDSC) copolymers

Copolymer	M_n (g/mol)		M_w/M_n[a]
	^{1}H NMR[b]	GPC[a]	
PEG-P(TMC-*co*-PDSC)	5,000–(3,980/2,850)	23,300	1.53
Mal-PEG-P(TMC-*co*-PDSC)	5,000–(3,980/2,980)	26,100	1.42

Notes: [a]M_n and M_w/M_n determined by GPC (eluent: DMF, flow rate: 1 mL/min, standards: polystyrene, 30°C). [b]M_n calculated from ^{1}H NMR.
Abbreviations: NMR, nuclear magnetic resonance; GPC, gel permeation chromatography; DMF, dimethylformamide.

Table 2 Characterization of MMP and cRGD-MMP micelles

Prodrug micelles	Drug loading content[a] (wt%)	Size[b] (nm)	PDI[b]
MMP	40.0	39	0.09
cRGD-MMP	40.3	45	0.11

Notes: [a]Calculated from ^{1}H NMR. [b]Polydispersed index (PDI), determined by DLS.
Abbreviations: MMP, micellar mertansine prodrug; cRGD-MMP, cRGD-functionalized micellar mertansine prodrug; NMR, nuclear magnetic resonance; DLS, dynamic light scattering.

In all, 5–6 week-old female nude mice (16–18 g) were provided by Beijing Vital River Laboratory Animal Technology (Beijing, China). The animals were housed at 25°C and 55% humidity under natural 12 h light/dark cycle conditions at the Experimental Animal Center of Soochow University. The mice were all handled under the guideline approved by the Soochow University Laboratory Animal Center. This research was approved by the Animal Care and Use Committee of Soochow University.

In vitro cytotoxicity of cRGD-MMP

The in vitro cytotoxicities of DM1, MMP and cRGD-MMP against MDA-MB-231 TNBCs were investigated by MTT assays. Briefly, MDA-MB-231 cells were grown in 96-well plates at 5×10^3 cells/well overnight. The different drug formulations at concentrations of 0.001355–13.55 μM were added. After 4 h, the medium was replaced by 100 μL fresh medium. The cells were cultured for another 44 h. In all, 20 μL of MTT solution (5 mg/mL) was added. The cells were further cultured for 4 h, the medium was removed and 150 μL of dimethyl sulfoxide (DMSO) was added to dissolve the MTT-formazan crystals. The absorbance of the above solution in each well was recorded using a microplate reader (Multiscan FC USD4600; Thermo Fisher Scientific) at 492 nm. The cell viability (%) was determined by comparing the absorbance at 492 nm with control wells containing only cell culture media. The results are presented as the mean ± standard deviation (n=4).

In vitro cellular targetability of cRGD-MMP

To study its targeting effect in vitro, cRGD-MMP was loaded with fluorescent DOX.[33] MDA-MB-231 cells were seeded on microscope slides at 4×10^4 cells/well in 400 μL cell culture medium overnight. DOX-loaded cRGD-MMP or MMP in 100 μL of phosphate-buffered saline (PBS; DOX concentration: 10 μg/mL) was added. After 4 or 8 h incubation, the cells were washed three times and fixed with 4 w/v% paraformaldehyde for 15 min at room temperature. The cells following washing three times with PBS, staining with DAPI, blue, and again washing three times with PBS were visualized using a confocal microscope (TCS-SP2; Leica Microsystems, Wetzlar, Germany).

In vivo imaging and biodistribution of cRGD-MMP

To assess the tumor-targeting efficacy of cRGD-MMP in vivo, the fluorescent dye DiR was encapsulated into cRGD-MMP and MMP. Typically, 0.2 mL of mixed dimethylformamide (DMF) solution (5 mg/mL) of PEG-P(TMC-*g*-SSDM1) and cRGD-PEG-P(TMC-*g*-SSDM1; w/w, 80/20) with 10 μL DiR solution (1 mg/mL, 1% DiR loading content) was added dropwise to 0.8 mL of PBS (10 mM, pH 7.4) and stirred for another 2 h, followed by extensive dialysis (Spectra/Por; molecular weight cut-off [MWCO] 7000) against PBS for 12 h. MDA-MB-231 triple-negative breast tumor xenograft model was established subcutaneously. In brief, ~2×10^6 MDA-MB-231 cells in 50 μL of serum-free DMEM media were subcutaneously inoculated into the hind flank of nude mice. When the tumor sizes reached 200–300 mm^3, 200 μL of DiR-loaded cRGD-MMP or MMP was intravenously administrated into the tail vein of tumor-bearing mice (dosage: 1 μg DiR equiv./mouse). At 0, 2, 4, 8, 12 or 24 h post injection, the fluorescence images of mice were acquired by the Maestro near-infrared fluorescence imaging system (CRi Inc., USA) with an excitation band filter at 748 nm and an emission at 780 nm.

The in vivo biodistribution studies were performed by tail vein injection of cRGD-MMP or MMP (dosage: 5 mg DM1 equiv./kg) to MDA-MB-231 tumor-bearing nude mice, and DM1 amounts in the tumor and major organs were quantified using the HPLC test. At 12 h post injection, the tumor and main organs containing heart, kidney, spleen, lung and liver were collected, washed with PBS, weighed, homogenized in methanol and extracted by DMF solution. The supernatants were treated with excess 1,4-dithio-D,L-threitol (50 mM) which followed centrifugation of the extracted solution at 18 krpm for 20 min. DM1 contents were quantified by the HPLC test. The results are presented as the mean ± standard deviation (n=3).

In vivo antitumor efficacy

The in vivo antitumor efficacy and safety of cRGD-MMP and MMP was investigated in MDA-MB-231 triple-negative breast tumor-bearing mice. In all, ~2×10^6 MDA-MB-231 cells in 50 μL of serum-free DMEM media were subcutaneously injected in the hind flank of nude mice. When the tumor sizes

reached ~70 mm^3 after inoculation, the mice were randomly divided into five groups (n=5). The mice were intravenously administrated with PBS, free DM1 at 0.8 mg/kg, MMP at 0.8 mg DM1 equiv./kg and cRGD-MMP at 0.8 or 1.6 mg DM1 equiv./kg, respectively, every two days for a total of four injections. Tumor sizes were recorded using calipers and calculated based on the following formula: $V = 0.5 \times L \times W^2$, where L and W are the longest and shortest tumor diameters.[34] The relative tumor volumes were normalized to the initial tumor volume when starting the treatment. The body weights of all mice were weighed every two days over the entire treatment period. At day 16, all mice were sacrificed, and tumors were harvested and weighed. Tumor inhibition rate (TIR) was calculated according to the following formula: (1 – mean tumor weight of drug treated group/mean tumor weight of saline treated group) ×100.

Hematoxylin and eosin (H&E) staining

At the end of the treatment, the mice were sacrificed and major organs, including liver, heart, spleen, lung and kidney, were excised. The tissues were fixed with 4% paraformaldehyde solution and embedded in paraffin. The sliced organ tissues (thickness: 4 μm) mounted on the glass slides were stained by H&E and observed by a digital microscope (Leica QWin; Leica Microsystems).

Results and discussion

Targetability and antitumor activity of cRGD-MMP toward MDA-MB-231 cells

We have shown previously that cRGD-MMP with a small size of 45 nm and high DM1 content of ~40 wt% can effectively target to $\alpha_v\beta_3$ integrin overexpressing B16F10 melanoma.[29] cRGD-MMP can also be used as a nanocarrier for other hydrophobic drugs like DTX to achieve synergistic melanoma chemotherapy.[35] Given the fact that MDA-MB-231 TNBC cells overexpress $\alpha_v\beta_3$ integrins and that ado-trastuzumab emtansine is clinically used for the treatment of HER2-positive metastatic breast cancers, we decided to investigate the targetability and treatment effect of cRGD-MMP toward MDA-MB-231 tumor. MTT assays showed that cRGD-MMP was highly potent against MDA-MB-231 cells in vitro with a low half-maximal inhibitory concentration (IC_{50}) of 0.18 μM, which was comparable to that of free DM1 (0.12 μM) and 2.2-fold lower than that of the nontargeted MMP control (0.39 μM; Figure 1), indicating that cRGD-MMP can target to MDA-MB-231 cancer cells and DM1 can be quickly released inside the cells. cRGD peptide-functionalized nanomedicines were reported to afford good targetability to MDA-MB-231 cells in vitro and in vivo.[36,37]

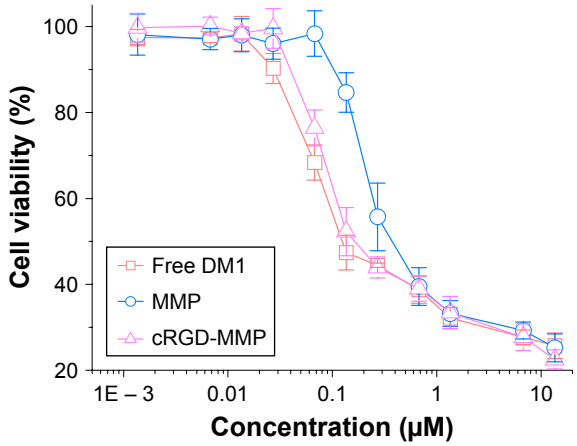

Figure 1 Viability of MDA-MB-231 cells following 48 h incubation with free DM1, cRGD-MMP or MMP at various DM1 concentrations.
Note: The results are presented as mean ± standard deviation (n=4).
Abbreviations: DM1, mertansine; cRGD-MMP, cRGD-functionalized micellar mertansine prodrug; MMP, micellar mertansine prodrug.

To visualize its intracellular delivery behavior in MDA-MB-231 cells, confocal studies were performed using cRGD-MMP loaded with 4.94 wt% DOX (a fluorescent anticancer drug). Dynamic light scattering (DLS) showed that DOX-loaded cRGD-MMP had a size of 41.0 nm. The results displayed that cells following 8 h treatment with DOX-loaded cRGD-MMP had much stronger intracellular DOX fluorescence than those with DOX-loaded MMP (nontargeted counterpart; Figure 2), supporting the active role of cRGD in mediating cellular uptake. It should be noted that the fluorescence of DOX could be self-quenched when encapsulated in the micelles resulting from homo-Förster resonance energy transfer (homo-FRET).[38,39] The observed strong DOX fluorescence in MDA-MB-231 cells confirms efficient internalization of cRGD-MMP by MDA-MB-231 cells and fast intracellular drug release.

In vivo imaging and biodistribution of cRGD-MMP

To assess their tumor targeting effect in vivo, cRGD-MMP and MMP micelles were loaded with DiR. The in vivo near-infrared fluorescence imaging showed strong DiR fluorescence in the tumor at 2 h following intravenous (i.v.) injection of cRGD-MMP (Figure 3). The tumor DiR fluorescence maximized at 12 h and remained strong even at 24 h. In comparison, DiR-loaded MMP (nontargeted control) gave much weaker tumor DiR fluorescence. These results signify that cRGD decoration of MMP can significantly enhance its accumulation in the MDA-MB-231 tumor in vivo.

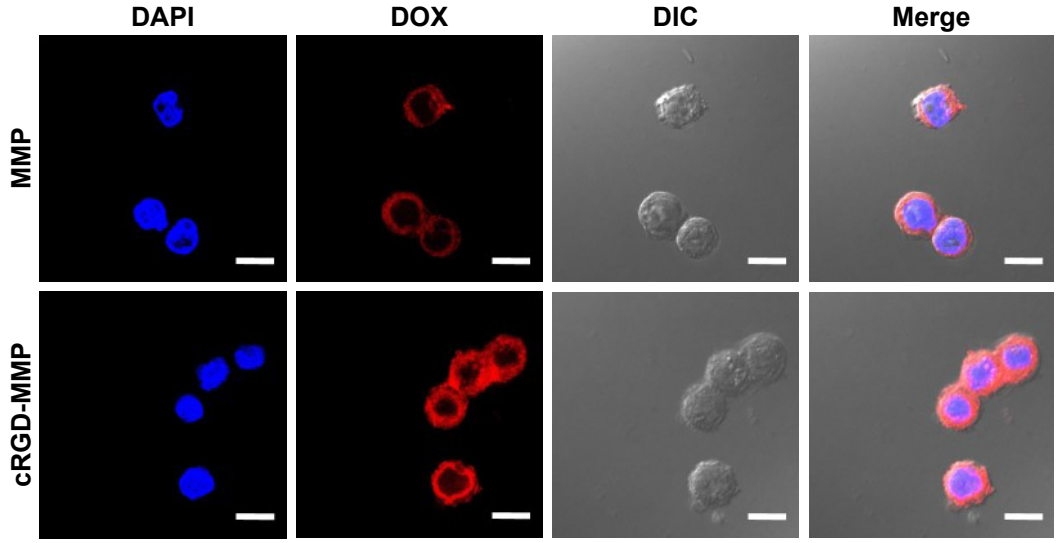

Figure 2 Confocal microscopy images of MDA-MB-231 cells following 8 h incubation with DOX-loaded cRGD-MMP or DOX-loaded MMP (10 μg DOX equiv./mL; scale bar: 10 μm).
Note: For each panel, the images from left to right show cell nuclei stained by DAPI (blue), DOX fluorescence in MDA-MB-231 cells (red), the DIC microscopy of cells and overlays of the three images.
Abbreviations: DOX, doxorubicin; cRGD-MMP, cRGD-functionalized micellar mertansine prodrug; MMP, micellar mertansine prodrug; DAPI, 4′6-diamidino-2-phenylindole dihydrochloride; DIC, differential interference contrast.

The in vivo biodistribution of cRGD-MMP and MMP was studied in MDA-MB-231 tumor-bearing nude mice. The mice were sacrificed at 12 h post injection of cRGD-MMP or MMP (dosage: 5 mg DM1 equiv./kg). The quantification of DM1 using HPLC measurements displayed that tumor uptake of DM1 was 8.10% of injected dose per gram of tissue (%ID/g) for cRGD-MMP, which was ~2.5-fold higher than that of nontargeted MMP control (Figure 4). Notably, similar uptake was observed for cRGD-MMP and MMP in the vital organs such as heart, liver, spleen, lung and kidney. The enhanced tumor accumulation of cRGD-MMP likely results from the specific affinity of cRGD peptide to the $\alpha_v\beta_3$ integrins that are overexpressed on tumor neovasculatures and MDA-MB-231 TNBCs.[40]

In vivo anticancer effect of cRGD-MMP

The in vivo therapeutic performance of cRGD-MMP was evaluated using MDA-MB-231 triple-negative breast

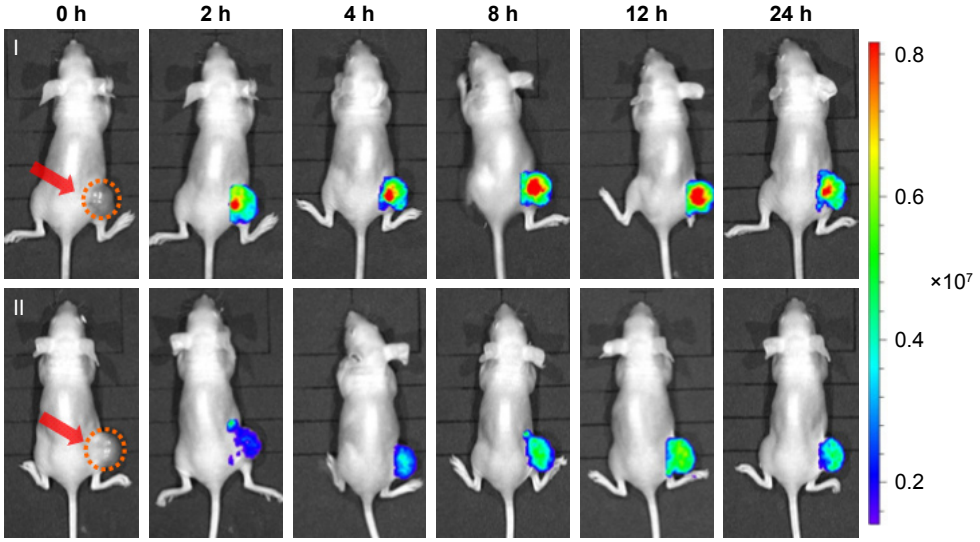

Figure 3 In vivo fluorescence imaging of MDA-MB-231 tumor-bearing mice after i.v. injection with DiR-loaded cRGD-MMP (I) or DiR-loaded MMP (II) (dosage: 1 μg DiR equiv./per mouse).
Note: The red arrows indicate the tumor region.
Abbreviations: i.v., intravenous; DiR, 1,1′-dioctadecyltetramethyl indotricarbocyanine iodide; cRGD-MMP, cRGD-functionalized micellar mertansine prodrug; MMP, micellar mertansine prodrug.

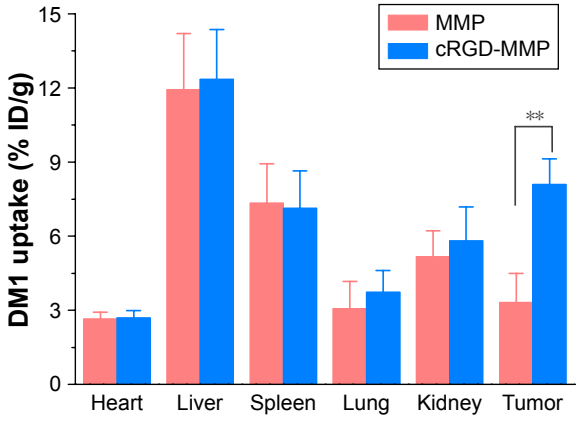

Figure 4 In vivo biodistribution of cRGD-MMP and MMP in MDA-MB-231 tumor-bearing mice at 12 h post i.v. injection (DM1 dosage: 5 mg/kg).
Notes: The results are presented as mean ± standard deviation (n=3). $^{**}p<0.01$ (Student's *t*-test).
Abbreviations: cRGD-MMP, cRGD-functionalized micellar mertansine prodrug; MMP, micellar mertansine prodrug; i.v., intravenous; DM1, mertansine; ID/g, injected dose per gram of tissue.

tumor-bearing mice. cRGD-MMP, MMP or free DM1 was administered every 3 days for a total of four injections at a dosage of 0.8 or 1.6 mg DM1 equiv./kg. As expected, mice treated with PBS showed rapid tumor growth (Figure 5A). Free DM1 showed modest tumor growth inhibition at 0.8 mg/kg. Considering that free DM1 has an maximum-tolerated dose of 1 mg/kg,[41] no higher dosage was attempted. cRGD-MMP exhibited better tumor suppression at 0.8 mg/kg than free DM1 and MMP controls under otherwise the same conditions. Moreover, cRGD-MMP showed a dose-dependent tumor growth inhibition, in which tumor progression was greatly enhanced at 1.6 mg DM1 equiv./kg. The images of tumors isolated on day 16 showed clearly that mice treated with cRGD-MMP at 1.6 mg DM1 equiv./kg had almost complete growth inhibition (Figure 5B). The tumor weights revealed that cRGD-MMP at 0.8 mg DM1 equiv./kg yielded a TIR of 67.3%, which was significantly higher than that for MMP (TIR: 46.2%) and free DM1 (TIR: 17.5%; Figure 5C). A high TIR of 87.6% was achieved with 1.6 mg DM1 equiv./kg cRGD-MMP. The significantly enhanced tumor growth inhibition of cRGD-MMP as compared to free DM1 is most likely because cRGD-MMP has a longer circulation time, better tumor selectivity and higher drug accumulation in tumor than free DM1. No obvious body weight loss was observed for all treatments over the entire

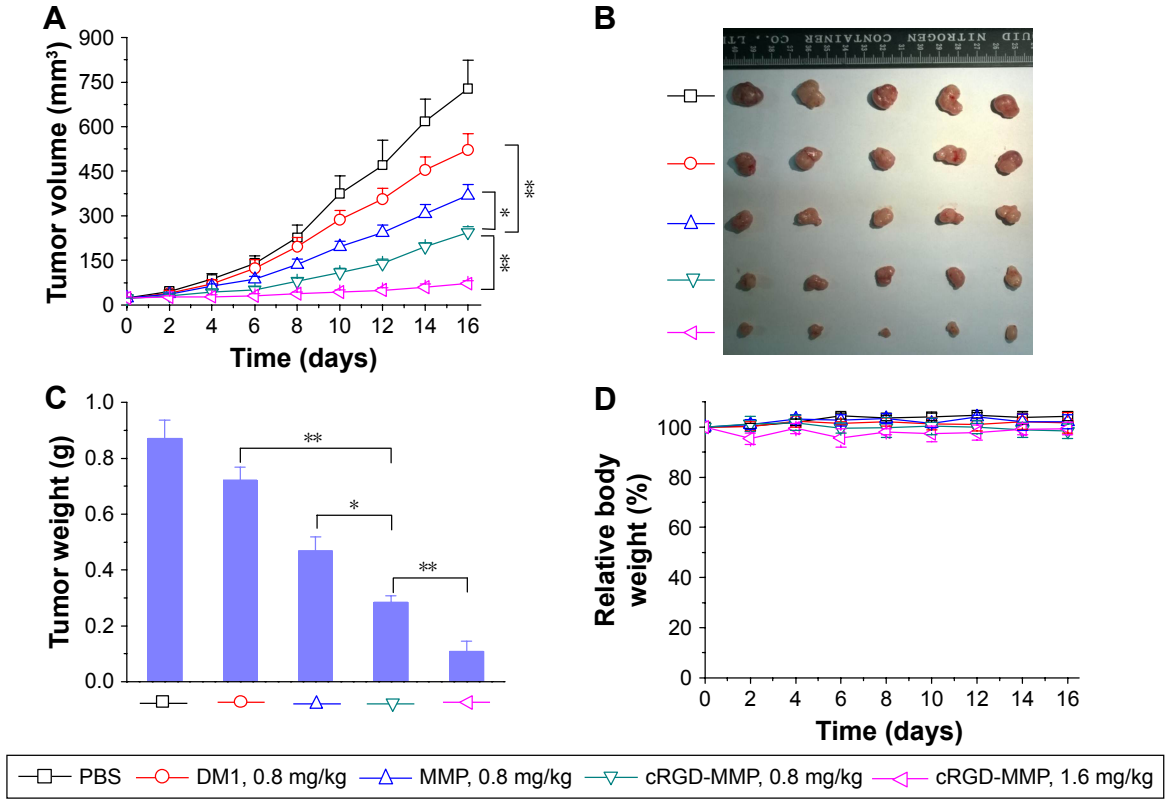

Figure 5 In vivo antitumor performance in subcutaneous MDA-MB-231 human triple-negative breast tumor-bearing nude mice.
Notes: (**A**) Tumor volume changes in MDA-MB-231 breast tumor-bearing mice treated with free DM1, MMP and cRGD-MMP. DM1 drugs were given on days 0, 3, 6 and 9 for a total of four injections. The results are presented as mean ± standard deviation (n=5). (**B**) Photographs of typical tumor blocks collected from different treatment groups on day 16. (**C**) Tumor weights of mice following 16 days treatment (n=5). (**D**) Change in mice body weights over 16 days following different treatments. $^{*}p<0.05$ and $^{**}p<0.01$ (ANOVA test).
Abbreviations: DM1, mertansine; MMP, micellar mertansine prodrug; cRGD-MMP, cRGD-functionalized micellar mertansine prodrug; ANOVA, analysis of variance; PBS, phosphate-buffered saline.

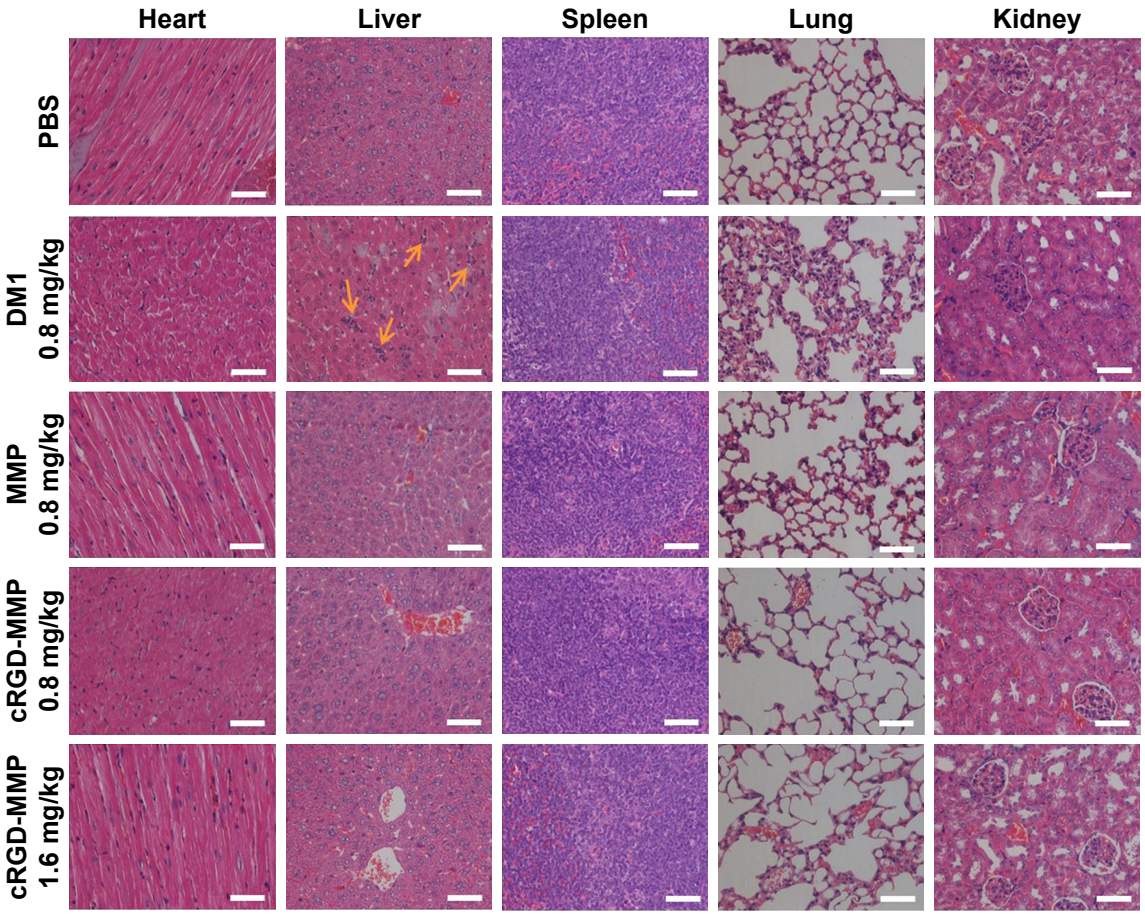

Figure 6 H&E staining of major organs of mice from different groups (scale bar: 50 μm).
Notes: The orange arrows in the liver tissue of group B indicate the obviously increased Kupffer cells, leading to liver damage. The images were acquired using Olympus BX41 microscope at 40× objective.
Abbreviations: H&E, hematoxylin and eosin; PBS, phosphate-buffered saline; DM1, mertansine; MMP, micellar mertansine prodrug; cRGD-MMP, cRGD-functionalized micellar mertansine prodrug.

experimental period (Figure 5D). Notably, formyl peptide receptor-targeting and paclitaxol-encapsulated human serum albumin nanoparticles were reported to cause more effective tumor inhibition though similar toxicity as compared to Taxol in MDA-MB-231 tumor-bearing mice.[42] Johnstone et al[43] reported that mitaplatin-loaded Poly (lactide-*co*-glycolide)-PEG nanoparticles with a long-term controlled drug release behavior exhibited a similar TIR to free mitaplatin in MDA-MB-468 tumor-bearing mice. DTX-loaded PEG-poly(epsilon-caprolactone) nanoparticles displayed a comparable in vivo antitumor efficacy and survival rate in MDA-MB-231 TNBC animal model to DTX commercial formulation (Taxotere®).[44] H&E staining displayed that cRGD-MMP at 0.8 and 1.6 mg DM1 equiv./kg did not cause significant damage to the major organs, while free DM1 induced obvious increased Kupffer cells in liver tissues, fat vacuoles, liver cell cord derangement and dilated intercellular spaces (Figure 6). All the abovementioned results demonstrate that cRGD-MMP has better tumor selectivity and enhanced treatment of MDA-MB-231 TNBC. These cRGD-decorated, polycarbonate-based, reduction-sensitive mertansine prodrug micelles have proven to be an effective platform for TNBC chemotherapy.

Conclusion

We have demonstrated that cRGD-MMP mediates highly potent and targeted treatment of $\alpha_v\beta_3$ integrin overexpressing MDA-MB-231 TNBC xenografts in nude mice. Notably, cRGD-MMP presents many great merits, including: 1) high affinity to MDA-MB-231 cells and fast intracellular drug release, leading to a potent antitumor effect comparable to free DM1; 2) high accumulation in the MDA-MB-231 tumor, reaching 8.1%ID/g at 12 h post injection, likely due to its high stability and active targeting ability; 3) significantly more effective inhibition of tumor growth than free DM1 and the nontargeted MMP controls at 0.8 mg DM1 equiv./kg; and 4) reduced systemic toxicity as compared to free DM1, which enables effective treatment of MDA-MB-231 tumor-bearing

mice at a higher dosage without causing obvious side effects. This MMP appears to be a promising platform for potent treatment of TNBCs.

Acknowledgments

This work was supported by the National Natural Science Foundation of China (NSFC 51373113 and 51633005) and the Natural Science Foundation of Jiangsu Province (BK20131166).

Author contributions

All authors contributed toward data analysis, drafting and revising the paper and agree to be accountable for all aspects of the work.

Disclosure

The authors report no conflicts of interest in this work.

References

1. Thomas A, Teicher BA, Hassan R. Antibody–drug conjugates for cancer therapy. *Lancet Oncol*. 2016;17(6):e254–e262.
2. Sievers EL, Senter PD. Antibody-drug conjugates in cancer therapy. *Annu Rev Med*. 2013;64:15–29.
3. Widdison WC, Wilhelm SD, Cavanagh EE, et al. Semisynthetic maytansine analogues for the targeted treatment of cancer. *J Med Chem*. 2006;49(14):4392–4408.
4. Chudasama V, Maruani A, Caddick S. Recent advances in the construction of antibody-drug conjugates. *Nat Chem*. 2016;8(2):114–119.
5. de Goeij BE, Lambert JM. New developments for antibody-drug conjugate-based therapeutic approaches. *Curr Opin Immunol*. 2016; 40:14–23.
6. Chari RV, Miller ML, Widdison WC. Antibody–drug conjugates: an emerging concept in cancer therapy. *Angew Chem Int Ed*. 2014;53(15): 3796–3827.
7. Verma S, Miles D, Gianni L, et al. Trastuzumab emtansine for HER2-positive advanced breast cancer. *N Engl J Med*. 2012;367(19): 1783–1791.
8. Amiri-Kordestani L, Blumenthal GM, Xu QC, et al. FDA approval: ado-trastuzumab emtansine for the treatment of patients with HER2-positive metastatic breast cancer. *Clin Cancer Res*. 2014;20(17): 4436–4441.
9. Shah MH, Lorigan P, O'Brien MER, et al. Phase I study of IMGN901, a CD56-targeting antibody-drug conjugate, in patients with CD56-positive solid tumors. *Invest New Drugs*. 2016;34(3):290–299.
10. Bosch A, Eroles P, Zaragoza R, Viña JR, Lluch A. Triple-negative breast cancer: molecular features, pathogenesis, treatment and current lines of research. *Cancer Treat Rev*. 2010;36(3):206–215.
11. Carey L, Winer E, Viale G, Cameron D, Gianni L. Triple-negative breast cancer: disease entity or title of convenience? *Nat Rev Clin Oncol*. 2010;7(12):683–692.
12. Abramson VG, Lehmann BD, Ballinger TJ, Pietenpol JA. Subtyping of triple-negative breast cancer: implications for therapy. *Cancer*. 2015; 121(1):8–16.
13. Clemons M, Danson S, Howell A. Tamoxifen ('Nolvadex'): a review: antitumour treatment. *Cancer Treat Rev*. 2002;28(4):165–180.
14. Hurvitz SA, Dirix L, Kocsis J, et al. Phase II randomized study of trastuzumab emtansine versus trastuzumab plus docetaxel in patients with human epidermal growth factor receptor 2-positive metastatic breast cancer. *J Clin Oncol*. 2013;31(9):1157–1163.
15. Marty M. Pertuzumab, trastuzumab, and docetaxel in HER2-positive metastatic breast cancer. *N Engl J Med*. 2015;372(8):724–734.
16. Mendes TFS, Kluskens LD, Rodrigues LR. Triple negative breast cancer: nanosolutions for a big challenge. *Adv Sci*. 2015;2(11):1500053.
17. Liedtke C, Mazouni C, Hess KR, et al. Response to neoadjuvant therapy and long-term survival in patients with triple-negative breast cancer. *J Clin Oncol*. 2008;26(8):1275–1281.
18. Uhm JE, Park YH, Yi SY, et al. Treatment outcomes and clinicopathologic characteristics of triple-negative breast cancer patients who received platinum-containing chemotherapy. *Int J Cancer*. 2009; 124(6):1457–1462.
19. Shi J, Kantoff PW, Wooster R, Farokhzad OC. Cancer nanomedicine: progress, challenges and opportunities. *Nat Rev Cancer*. 2017; 17(1):20–37.
20. Xu X, Ho W, Zhang X, Bertrand N, Farokhzad O. Cancer nanomedicine: from targeted delivery to combination therapy. *Trends Mol Med*. 2015;21(4):223–232.
21. Zhong Y, Meng F, Deng C, Zhong Z. Ligand-directed active tumor-targeting polymeric nanoparticles for cancer chemotherapy. *Biomacromolecules*. 2014;15(6):1955–1969.
22. Kutty RV, Feng S-S. Cetuximab conjugated vitamin E TPGS micelles for targeted delivery of docetaxel for treatment of triple negative breast cancers. *Biomaterials*. 2013;34(38):10160–10171.
23. Kutty RV, Chia SL, Setyawati MI, Muthu MS, Feng S-S, Leong DT. In vivo and ex vivo proofs of concept that cetuximab conjugated vitamin E TPGS micelles increases efficacy of delivered docetaxel against triple negative breast cancer. *Biomaterials*. 2015;63:58–69.
24. Paulmurugan R, Bhethanabotla R, Mishra K, et al. Folate receptor–targeted polymeric micellar nanocarriers for delivery of orlistat as a repurposed drug against triple-negative breast cancer. *Mol Cancer Ther*. 2016;15(2):221–231.
25. Brinkman AM, Chen G, Wang Y, et al. Aminoflavone-loaded EGFR-targeted unimolecular micelle nanoparticles exhibit anti-cancer effects in triple negative breast cancer. *Biomaterials*. 2016;101:20–31.
26. Andey T, Sudhakar G, Marepally S, Patel A, Banerjee R, Singh M. Lipid nanocarriers of a lipid-conjugated estrogenic derivative inhibit tumor growth and enhance cisplatin activity against triple-negative breast cancer: pharmacokinetic and efficacy evaluation. *Mol Pharm*. 2015; 12(4):1105–1120.
27. Hu G, Chun X, Wang Y, He Q, Gao H. Peptide mediated active targeting and intelligent particle size reduction-mediated enhanced penetrating of fabricated nanoparticles for triple-negative breast cancer treatment. *Oncotarget*. 2015;6(38):41258–41274.
28. Wu K, Cheng R, Zhang J, Meng F, Deng C, Zhong Z. Micellar nanoformulation of lipophilized bortezomib: high drug loading, improved tolerability and targeted treatment of triple negative breast cancer. *J Mater Chem B*. 2017;5:5658–5667.
29. Zhong P, Meng H, Qiu J, et al. αvβ3 Integrin-targeted reduction-sensitive micellar mertansine prodrug: superb drug loading, enhanced stability, and effective inhibition of melanoma growth in vivo. *J Control Release*. 2017;259:176–186.
30. Chen H, Zhang X, Dai S, et al. Multifunctional gold nanostar conjugates for tumor imaging and combined photothermal and chemo-therapy. *Theranostics*. 2012;3(9):633–649.
31. Murugan C, Rayappan K, Thangam R, et al. Combinatorial nanocarrier based drug delivery approach for amalgamation of anti-tumor agents in breast cancer cells: an improved nanomedicine strategies. *Sci Rep*. 2016;6:34053–34069.
32. Othman BA, Greenwood C, Abuelela AF, et al. Correlative light-electron microscopy shows RGD-targeted ZnO nanoparticles dissolve in the intracellular environment of triple negative breast cancer cells and cause apoptosis with intratumor heterogeneity. *Adv Healthc Mater*. 2016;5(11):1310–1325.
33. Zhong Y, Goltsche K, Cheng L, et al. Hyaluronic acid-shelled acid-activatable paclitaxel prodrug micelles effectively target and treat CD44-overexpressing human breast tumor xenografts in vivo. *Biomaterials*. 2016;84:250–261.

34. Liu S, Liu J, Ma Q, et al. Solid tumor therapy by selectively targeting stromal endothelial cells. *Proc Natl Acad Sci U S A*. 2016;113(28):E4079–E4087.
35. Zhong P, Qiu M, Zhang J, et al. cRGD-installed docetaxel-loaded mertansine prodrug micelles: redox-triggered ratiometric dual drug release and targeted synergistic treatment of B16F10 melanoma. *Nanotechnology*. 2017;28:295103.
36. Liu P, Qin L, Wang Q, et al. cRGD-functionalized mPEG-PLGA-PLL nanoparticles for imaging and therapy of breast cancer. *Biomaterials*. 2012;33(28):6739–6747.
37. Jin G, Feng G, Qin W, Tang BZ, Liu B, Li K. Multifunctional organic nanoparticles with aggregation-induced emission (AIE) characteristics for targeted photodynamic therapy and RNA interference therapy. *Chem Commun*. 2016;52(13):2752–2755.
38. Zhu Y, Zhang J, Meng F, et al. cRGD-functionalized reduction-sensitive shell-sheddable biodegradable micelles mediate enhanced doxorubicin delivery to human glioma xenografts in vivo. *J Control Release*. 2016;233:29–38.
39. Kobayashi H, Choyke PL. Target-cancer-cell-specific activatable fluorescence imaging probes: rational design and in vivo applications. *Acc Chem Res*. 2011;44(2):83–90.
40. Song W, Tang Z, Zhang D, et al. Anti-tumor efficacy of c(RGDfK)-decorated polypeptide-based micelles co-loaded with docetaxel and cisplatin. *Biomaterials*. 2014;35(9):3005–3014.
41. Zhong P, Zhang J, Deng C, Cheng R, Meng F, Zhong Z. Glutathione-sensitive hyaluronic acid-SS-mertansine prodrug with a high drug content: facile synthesis and targeted breast tumor therapy. *Biomacromolecules*. 2016;17(11):3602–3608.
42. Liu L, Bi Y, Zhou M, et al. Biomimetic human serum albumin nanoparticle for efficiently targeting therapy to metastatic breast cancers. *Acs Appl Mater Interfaces*. 2017;9(8):7424–7435.
43. Johnstone TC, Kulak N, Pridgen EM, Farokhzad OC, Langer R, Lippard SJ. Nanoparticle encapsulation of mitaplatin and the effect thereof on in vivo properties. *ACS Nano*. 2013;7(7):5675–5683.
44. Palma G, Conte C, Barbieri A, et al. Antitumor activity of PEGylated biodegradable nanoparticles for sustained release of docetaxel in triple-negative breast cancer. *Int J Pharm*. 2014;473(1–2):55–63.